Recent Applications of Nuclear Track Emulsion Technique

P. I. Zarubin[a,b]*

[a] Veksler and Baldin Laboratory of High Energy Physics, Joint Institute for Nuclear Research, Dubna, 141980 Russia
[b] Lebedev Physical Institute, Russian Academy of Sciences, Moscow, 119991 Russia
*e-mail: zarubin@lhe.jinr.ru

Abstract—A survey of recent results obtained using the nuclear track emulsion (NTE) technique in low energy applications is given. NTE irradiation with 60 MeV ^{8}He nuclei provides identification of their decays at stopping, evaluation of the possibility of α range spectrometry, and observation of drift of thermalized ^{8}He atoms. Correlations of α particles studied in ^{12}C $\rightarrow$ 3α splitting induced by 14.1 MeV neutrons indicate the presence of a superposition of 0^+ and 2^+ states of the ^{8}Be nucleus in the ground state of ^{12}C. Angular correlations of fragments are studied in boron-enriched NTE, and the prospects of NTE application in radioactivity and nuclear fission research are discussed. It is proposed to use an automated microscope to search for collinear tripartition of heavy nuclei implanted in NTE. Surface irradiation of NTE by a ^{252}Cf source is started. Planar events containing fragment pairs and long range α particles, as well as fragment triples, are studied. NTE samples are calibrated using Kr and Xe ions with an energy of 1.2 and 3 A MeV.

INTRODUCTION

In spite of the fact that nuclear track emulsion (NTE) was developed half a century ago, it still remains a universal and cost-efficient detector [1−3]. NTE of BR-2 type with an unsurpassed spatial resolution of about 0.5 μm provides track observation beginning from fission fragments up to relativistic particles. The NTE technique deserves further application in fundamental and applied research at modern accelerators and reactors, as well as with radioactivity sources, including natural ones. The application of NTE is especially well grounded in such pioneering experiments where tracks of nuclear particles cannot be reconstructed using electronic detectors. Thus, in the last decade, the NTE technique applied in the framework of the BECQUEREL project [4] at the Nuclotron (JINR) allowed one to study with unique completeness clusterization in ^{7}Li, ^{7,9}Be, ^{8,10}B, ^{9,10}C, and ^{12,14}N nuclei at their relativistic dissociation in NTE [5].

Production of NTE layers in Moscow that had lasted for forty years stopped ten years ago. The interest in further application of NTE stimulated its reproduction at the workshop MIKRON, which is a part of the Slavich Company (Pereslavl-Zalessky) [6]. At present, NTE samples are produced by casting layers from 50 to 200 μm onto a glass substrate. Substrate-free layers with a thickness of up to 500 μm have become available recently. The testing of the new NTE via irradiation with relativistic particles proved its similarity to NTE BR-2.

The competitive character of NTE was proved not long ago in a series of measurements of short tracks of α particles and heavy ions using the highest precision optical microscopes KSM with 500× objectives. The possibility of α spectrometry was verified and the ^{8}He atom drift effect was established in measurement of decays of ^{8}He nuclei implanted in NTE [7−9]. Correlations of α particle trios in fission of ^{12}C nuclei from NTE by 14.1 MeV neutrons [10], as well as angular correlations of ^{7}Li and ^{4}He nuclei produced in ^{10}B breakup by thermal neutrons in boron-enriched NTE [11], were studied. In this series of experiments, the NTE angular resolution proved to be perfect, as the expected physical effects in opening angle distributions of reaction products under study could be clearly observed.

Samples of reproduced NTE were also irradiated with muons with an energy of 160 GeV [11]. Such irradiation allows one to study multifragmentation under the action of an electromagnetic probe. Multiphoton exchange or virtual photon−meson transformations can serve as the fragmentation mechanisms. It was established that the breakup of carbon nuclei into trios of α particles has a nuclear diffraction rather than electromagnetic character. It is important to prove this conclusion not only for interpretation of multifragmentation under the action of ultrarelativistic muons. It can also be the basis for interpretation of multifrag-
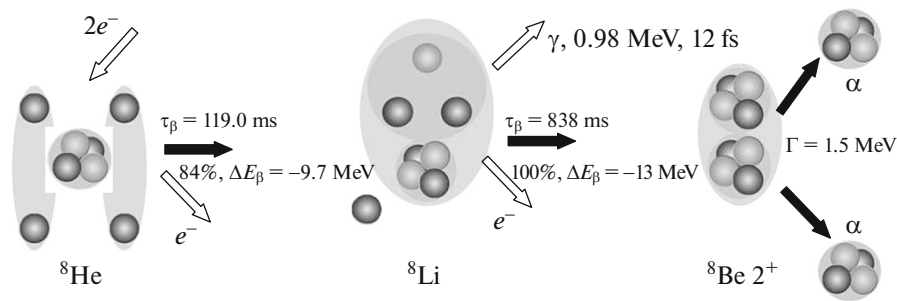
Fig. 1. Schematic diagram of the main channel of ^{8}He cascade decays: light circles correspond to protons; dark circles correspond to neutrons.

mentation of relativistic nuclei in peripheral interactions not accompanied by fragmentation of target nuclei. Thus, the connection of high energy and low energy nuclear physics appears.

One of the proposed tasks is the search for collinear cluster tripartition of heavy nuclei [12]. The existence of this phenomenon can be established in observation of such type of tripartition of heavy nuclei in which the lightest fragment is emitted in the direction of one of the heavy fragments. In spite of certain observability of fission fragments, they cannot be completely identified in NTE. The advantage of NTE is the combination of the best angular resolution and maximum sensitivity. Moreover, it is possible to measure the track length and thickness and thus classify fragments. At the initial stage, in order to provide trial statistics of tripartitions, it was proposed to analyze large areas of NTE irradiated by an ^{252}Cf source with appropriate density of α-particle tracks and fragments of spontaneous fission [13]. Further on, NTE layers enriched by ^{235}U would be irradiated with thermal neutrons. This approach can be developed for NTE enriched in ^{252}Cf [14, 15].

At high energies, the reproduced emulsion was irradiated at the Nuclotron (JINR) by the secondary ^{11}C nuclear beam with an energy of $1.2\,A$ GeV [16]; this allows one to include clusterization of this nucleus in the general pattern for the data on light nuclei, including radioactive ones. In spring, 2016, NTE layers were irradiated with ^{12}C nuclei with an energy of $450\,A$ MeV from the beam for medical and biological applications of the Institute for High Energy Physics (Protvino). In this case, a tungsten converter was installed in front of the irradiated NTE files for enhancing the electromagnetic effect.

This summarizes the studies with irradiation of new NTE samples in 2012–2016. The published results obtained on the basis of these data are summarized below.

STOPPED ^{8}He NUCLEI

NTE emulsions were irradiated with ^{8}He nuclei with an energy of 60 MeV [7–9] at the fragment separator ACCULINNA of the Flerov Laboratory of Nuclear Reactions (JINR). The specific features of ^{8}He isotope decay are shown in Fig. 1 [17]. Figure 2 shows macrophotos of "hammer-like" decays of ^{8}He nuclei stopped in NTE. These are typical decays among about two thousand observed in this study. Video records of these decays obtained using a microscope and a digital camera have been stored [18].

The search for β decays of ^{8}He nuclei was concentrated on the search for "hammers." Often, gaps were observed between the stopping points of primary tracks and the "hammer-like" decays in the so-called "broken" events. "Broken" events were assumed to take place owing to drift of the produced ^{8}He atoms. The directions of ^{8}He arrival, the stopping points of their nuclei, the vertices of their decay, and the stopping points of α particles were detected for 136 "whole" and 142 "broken" events. In "broken" events, the decay points were determined by extrapolation of electron tracks. The distribution of opening angles for α-particle pairs has an average value of $(164.9 \pm 0.7)°$. Such "hammer" kinks are connected with momenta carried away by $e\nu$ pairs.

The connection between α-particle ranges and energies was determined via spline interpolation of calculations using SRIM [19]. The energies and opening angles of α particles yield the α-decay energy distribution $Q_{2\alpha}$. The invariant variable Q is determined as the difference between the invariant mass of the final system M^* and the mass of the primary nucleus M. M^* is determined as the sum of products of four-momenta P_i, i.e., $M^{*2} = (\sum P_i)^2$.

The $Q_{2\alpha}$ distribution (Fig. 3) on the whole corresponds to the decay from the first excited state of ^{8}Be$_{2+}$. For events in which the ranges of both α particles are shorter than 12.5 μm and the opening angles are larger than 145°, the average value of $Q_{2\alpha}$ is equal to (2.9 ± 0.1) MeV with the RMS equal to 0.85 MeV, which corresponds to ^{8}Be$_{2+}$. At the same time, this
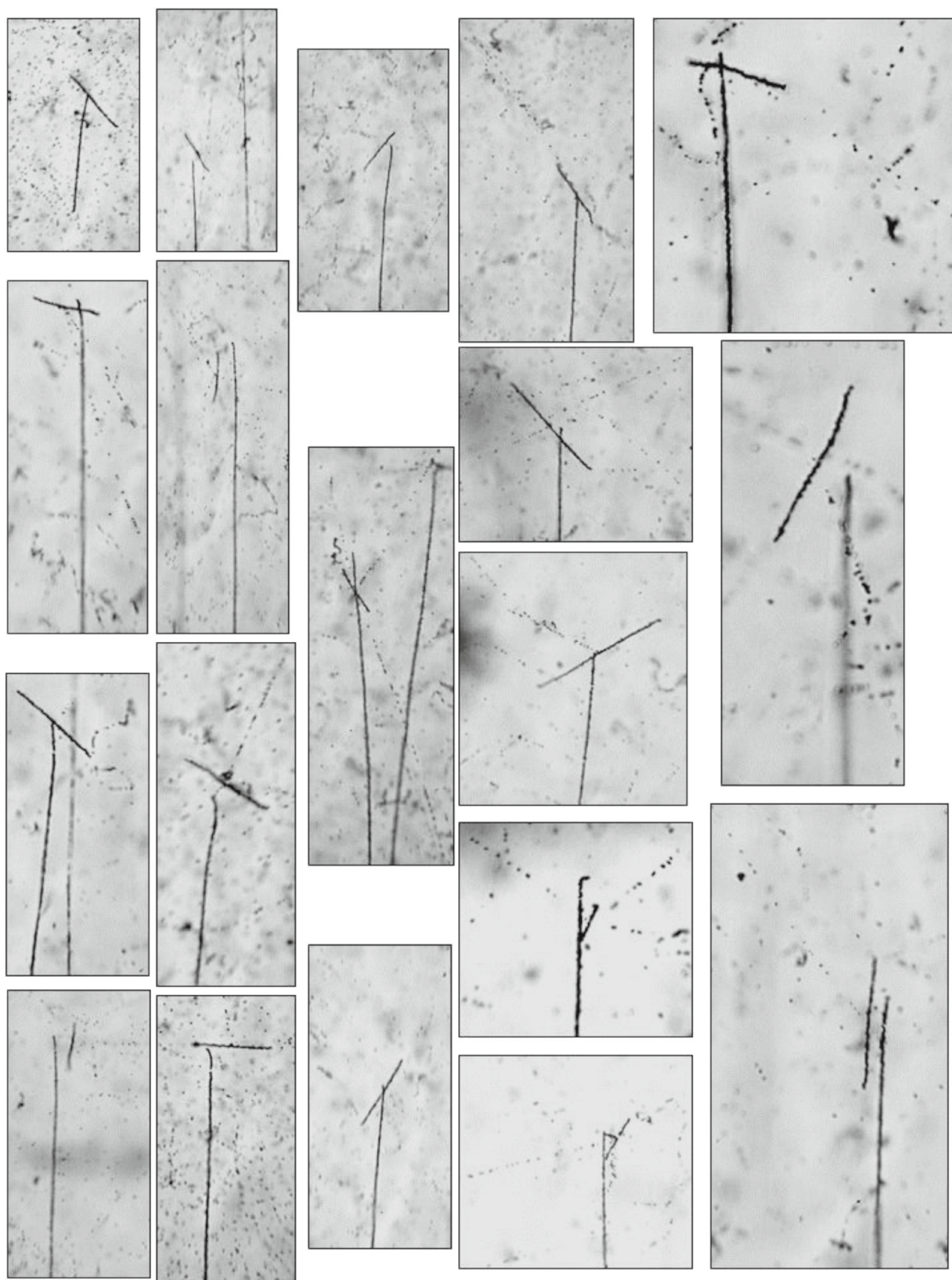
Fig. 2. Macrophotos of "hammer-like" decays of ^{8}He nuclei stopped in NTE: beginning at the bottom, ^{8}He tracks are oriented vertically; short tracks correspond to ^{8}Be$_{2+}$ decays; pointlike tracks are those of decay electrons.
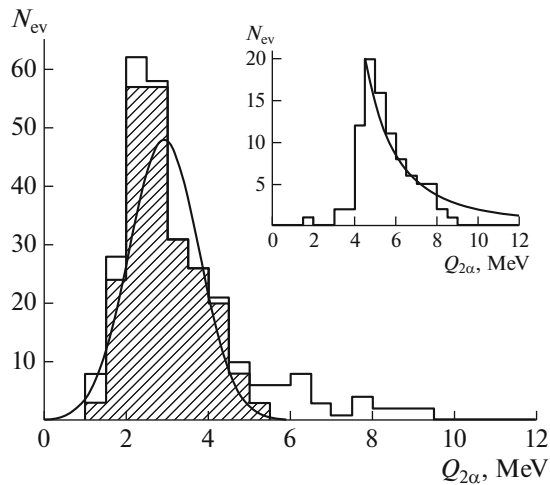
Fig. 3. Energy $Q_{2\alpha}$ distribution for 278 pairs of α particles: shaded histogram corresponds α particles with ranges shorter than 12.5 μm; line corresponds to the Gaussian approximation; the inset shows the $Q_{2\alpha}$ distribution of 98 additional pairs with α-particle ranges above 12.5 μm.

distribution has an extended "tail" which is not described by a Gaussian. The inset in Fig. 3 shows the $Q_{2\alpha}$ distribution corresponding to both ranges longer than 12.5 μm. The physical reason for this "tail" in the $Q_{2\alpha}$ distribution remains unclear. It is possible that its shape reflects the spatial structure of the $^8Be_{2+}$ state.

The distances $L(^8He-^8Be)$ between the stopping points of ^8He ions and the decay vertices and the angles $\Theta(^8He-^8Be)$ between the ion incidence and the

line connecting the stopping points and the decay vertices were determined in "broken" events (Fig. 4). The distribution homogeneity for these parameters and the absence of pronounced correlations point to thermal drift of ^8He atoms. The average value of $L(^8He-^8Be)$ equal to (5.8 ± 0.3) μm with the RMS of 3.1 μm can be associated with the average range of ^8He atoms. The low average velocity of ^8He atoms determined as the ratio of the average value $L(^8He-^8Be)$ and the half-life of ^8He nucleus points to the diffusion pattern.

It is interesting to study angular $\beta\beta$ correlations for the search for polarization conservation for intermediate ^8Li nuclei as the next step. The observed diffusion indicates the possibility of generating and pumping out radioactive ^8He atoms as an idea for the future. It is possible to increase the average velocity and drift range if the target is heated and its density is reduced. Then it is possible to accumulate a substantial amount of ^8He atoms. Of applied interest is the investigation of thin filters by pumping ^8He atoms and implanting these atoms into α detectors.

^{12}C NUCLEI SPLITTING INTO TRIOS OF α PARTICLES BY FUSION NEUTRONS

The ^{12}C nucleus is a recognized "starting point" in the concept of α-particle clusterization. It can be assumed that the $^{12}C_{g.s.}$ ground state contains a pair of virtual α clusters (beyond the mass surface), each possessing two units of orbital angular momentum (D waves) corresponding to the first excited state of $^8Be_{2+}$. "Rotation" of the two α clusters in the opposite direc-
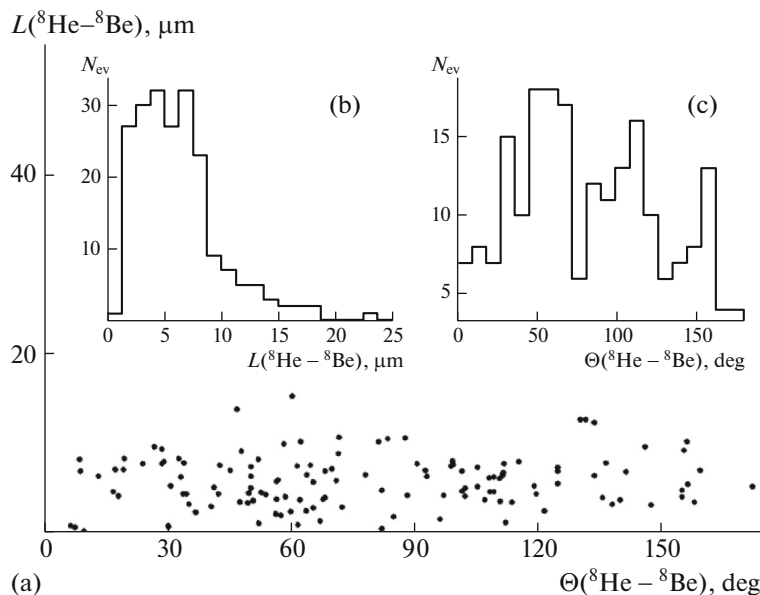

Fig. 4. Event distribution with respect to the distances $L(^8He-^8Be)$ and angles $\Theta(^8He-^8Be)$; the insets show projections (b) $L(^8He-^8Be)$ and (c) Θ ($^8He-^8Be$).
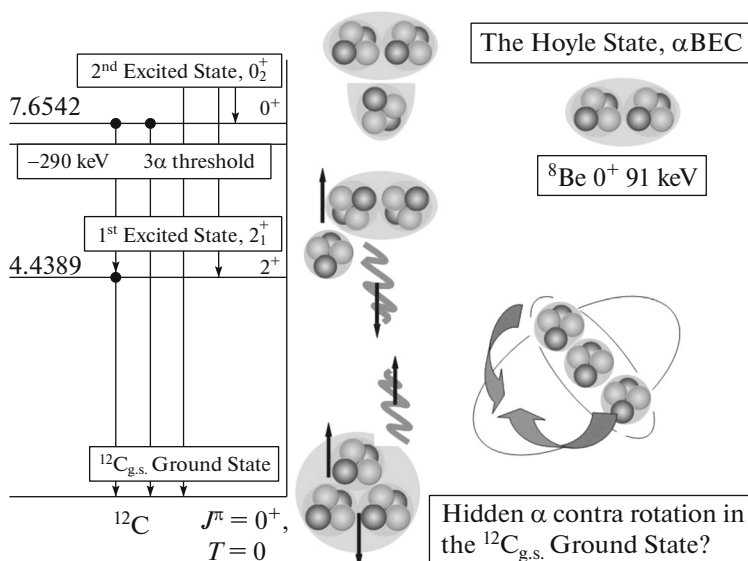
Fig. 5. Diagram of ^{12}C synthesis in 3α process.

tions about the common center represented by the third α cluster can be attributed to the ground state of $^8\text{Be}_{\text{g.s.}}$ (S wave). As a result, superposition of triple pairing results in the zero spin of $^{12}\text{C}_{\text{g.s.}}$. This simplified classical pattern can be manifested in intense production of unstable states in ^{12}C nuclei splitting.

This concept does not contradict the scenario of ^{12}C synthesis accepted in astrophysics (Fig. 5). The trio of α particles can undergo fusion when it is in the second excited state 0_2^+ of ^{12}C nucleus (the Hoyle state). This state, 270 keV above the $^{12}\text{C} \rightarrow 3\alpha$ decay threshold, can be considered as the triple superposition of $^8\text{Be}_{\text{g.s.}}$, since each of the α particle pairs is above the binding threshold by 90 keV, similar to $^8\text{Be}_{\text{g.s.}}$. The transition into the first excited (bound) state of ^{12}C nucleus takes place via emission of the photon carrying away two units of angular momentum of the trio $(0_2^+ \rightarrow 2_1^+)$. Thus, the D-wave α pair is formed in the trio as a result of angular momentum conservation. The subsequent transition to $^{12}\text{C}_{\text{g.s.}}$, also accompanied by a photon emission, results in formation of another D-wave α pair. This pair should have angular momentum with the direction opposite to the first pair in order to ensure zero spin of $^{12}\text{C}_{\text{g.s.}}$. Thus, the ^{12}C nucleus acquires hidden polarization. Figuratively speaking, it preserves "hidden rotation."

It can be assumed that emission of α-particle pairs via $^8\text{Be}_{2+}$ and $^8\text{Be}_{\text{g.s.}}$ states in reactions not accompanied by angular momentum transfer reflects such $^{12}\text{C}_{\text{g.s.}}$ spin cluster structure. The investigation of α-particle trios is possible in decay of carbon nuclei from NTE by 14.1 MeV neutrons. The energy transmitted to α particles is sufficient for measurement of their

ranges and directions, remaining below the threshold of background channels. A file of NTE layers on glass was irradiated with neutrons produced in the $d + t \rightarrow n + \alpha$ reaction at one of the DVIN installations for applied use [20]. Layers were scanned with the aim of searching for 3α decays. For 400 α trios selected from 1200 events, α-particle emission angles with respect to the NTE plane and their ranges were measured using the KSM microscope. The only criterion for event selection was the completeness of its measurement.

The angles and energies determined from ranges using SRIM allow one to determine the pair energy $Q_{2\alpha}$. The energy $Q_{2\alpha}$ and opening angle $\Theta_{2\alpha}$ correlation in α-particle pairs indicates the presence of ^{8}Be (Fig. 6). The domain with large opening angles $\Theta_{2\alpha} > 90°$ corresponds to $Q_{2\alpha}$ for $^8\text{Be}_{2+}$, and the one with $\Theta_{2\alpha} < 40°$ corresponds to $^8\text{Be}_{\text{g.s.}}$. The $Q_{2\alpha}$ event distribution indicates the presence of both states (Fig. 7), somewhat smeared, however, owing to the cluster knockout by neutrons. The soft condition $Q_{2\alpha} < 500$ keV provides 110 $^8\text{Be}_{\text{g.s.}}$ decays. The $^8\text{Be}_{\text{g.s.}}$ selection results in the visualization of the second peak in the region of $^8\text{Be}_{2+}$. Thus, in spite of the complex mechanism of the $^{12}\text{C}(n,n)3\alpha$ reaction, the existence of the virtual configuration $^8\text{Be}_{2+} + ^8\text{Be}_{2+} + ^8\text{Be}_{\text{g.s.}}$ in the ground state of ^{12}C is manifested in one-fourth of 3α decays.

The importance of the structure under discussion is determined by the interest in description of $^{12}\text{C}_{\text{g.s.}}$, as well as the fact that it is the initial configuration for the inverse process of 3α-particle ensemble generation in the Hoyle state. It is assumed that, following $^8\text{Be}_{\text{g.s.}}$, it represents a Bose–Einstein condensate consisting of α particles in the S state [21]. Its detection in decay of ^{12}C nuclei in which all pairs correspond to $^8\text{Be}_{\text{g.s.}}$
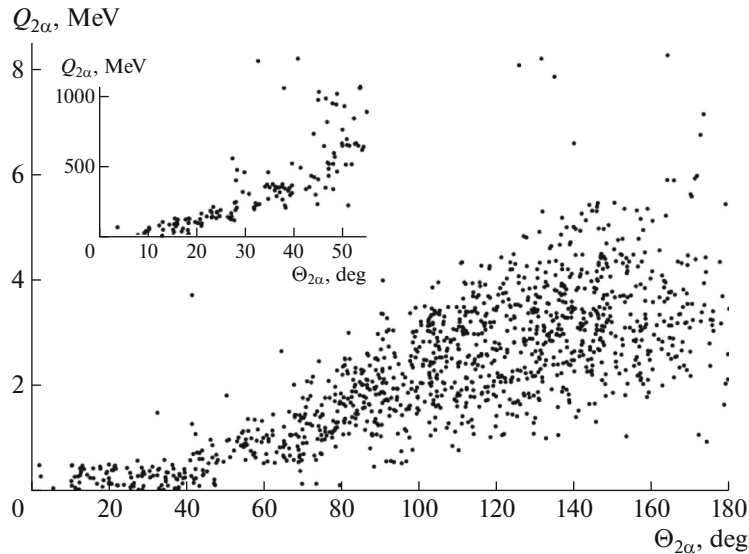
Fig. 6. Energy $Q_{2\alpha}$ and opening angle $\Theta_{2\alpha}$ correlations in α-particle pairs.

makes a step toward generation of condensate states with a large number of α particles. The fundamental idea of reproduction of such a condensate is the requirement to "evacuate" two hidden rotations in $^{12}C_{g.s.}$. In this regard, Coulomb dissociation of a fast moving nucleus on a heavy target nucleus seems the most appropriate process, since it allows exchange of several quasi-real photons.

CALIBRATION BY HEAVY IONS

NTE samples were irradiated at the Flerov Laboratory of Nuclear Reactions (JINR) at the IC-100 cyclotron with $^{86}Kr^{+17}$ and $^{124}Xe^{+26}$ ions with an energy of $1.2\,A$ MeV and at the U-400M cyclotron with ^{84}Kr ions

Fig. 7. Energy $Q_{2\alpha}$ distribution of α-particle pairs produced in ^{12}C nuclei decays by 14 MeV neutrons: (solid line) all α pairs, (shaded) selected $^{8}Be_{g.s.}$, and (dashed line) their difference.

with an energy of $3\,A$ MeV. The irradiation was performed in vacuum without a black paper. Samples were mounted in irradiation chambers with photolamps as the light sources. For better track observation, samples were installed at a large angle with respect to the beams. The sample irradiation density reached 10^6 tracks/cm^2 in several seconds. Figure 8 shows the range distribution for ions stopped in NTE without visible scattering. These data are important for further NTE calibration at lower energies typical of splitting of heavy nuclei.

IRRADIATION BY A Cf SOURCE

Surface irradiations of NTE samples at the Department of Radiation Dosimetry of the Nuclear Physics Institute (Academy of Sciences of the Czech Republic, Prague) were performed at first with manual movement of the ^{252}Cf source. Then a specially developed device was applied; the source was moved over the surface of this device automatically according to a convenient space and time pattern. The most probable is isotope ^{252}Cf decay with emission of α particles with an energy of 5–6 MeV; tracks of these α particles mainly fill the irradiated sample. This isotope can also undergo spontaneous fission into two or even three fragments with a probability of 3% and 0.1%, respectively. The NTE sample was irradiated by an ^{241}Am source emitting α particles alone in the same energy range for comparison. Since the ranges of decay products are short, the irradiations were performed without a black paper in a darkroom illuminated by red light.

In the case of surface irradiation, not more than two fission fragments should be observed, since the third one is emitted toward the contacting source. The specific feature of irradiation with ^{252}Cf is tracks of α
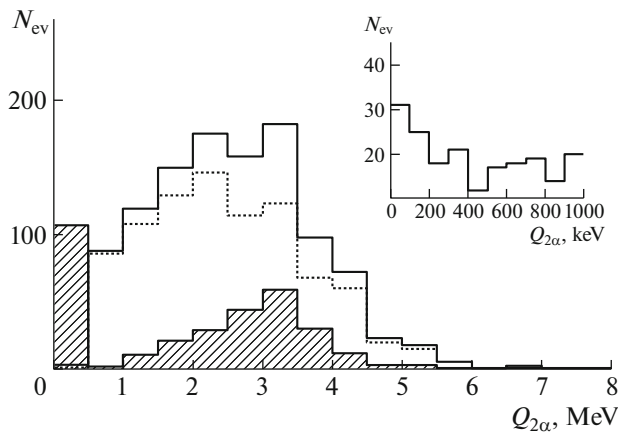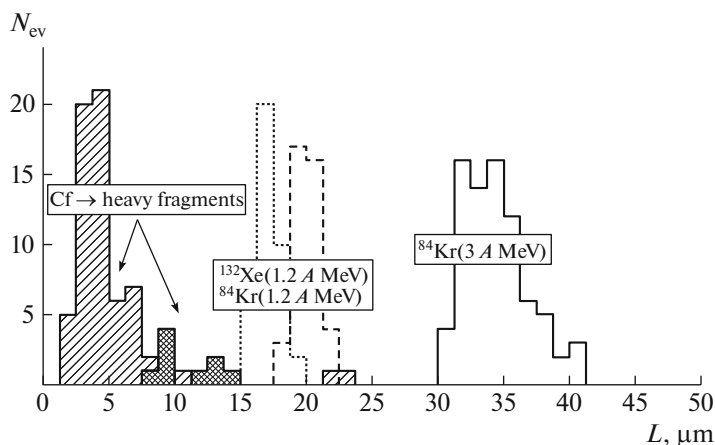
Fig. 8. ^{84}Kr, ^{132}Xe, and ^{86}Kr ion range distributions in decays Cf → 3 fragments and Cf → 2 fragments + long-range α.
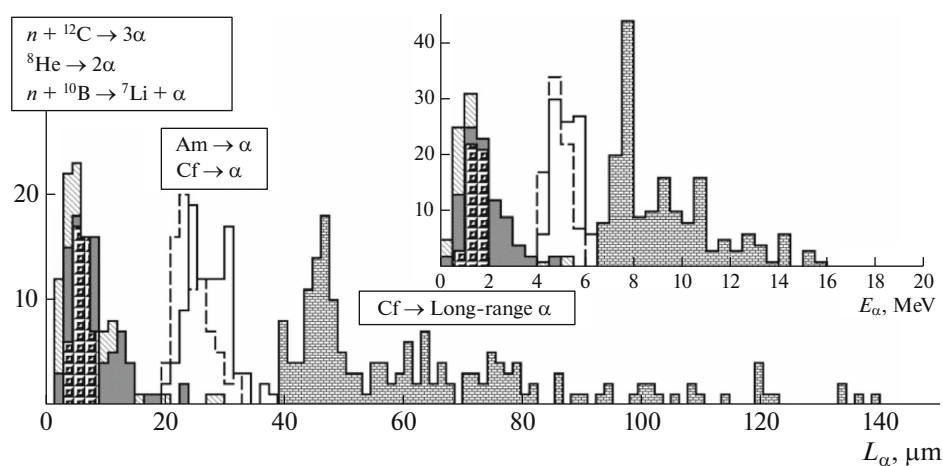
Fig. 9. Distributions of α-particle ranges: (hatching) n(14.1 MeV) + ^{12}C → 3α, (gray shading) ^{8}He → 2α, (solid dots) n_{th} + ^{10}B → ^{7}Li + α, (solid line) Cf → α, (dashed line) Am → α, (dark shading) Cf → long range α; inset: α-particle energy distribution estimated via spline interpolation of range−energy calculation SRIM.

particles from tripartition whose ranges considerably exceed the ranges of decay α particles. This channel dominates in tripartition of ^{252}Cf with a probability of 90%. Figure 9 shows the measured α-particle ranges in the above experiments. The energy values in the inset to Fig. 9 were calculated using SRIM [19].

When the NTE surface irradiated by the Cf source was examined, planar trios consisting of pairs of fragments and long-range α particles and trios of fragments were found (see Fig. 10). It should be underlined that the fact of observation of trios in NTE, rather than just pairs of fragments, is quite remarkable. For this to be possible, the vertices of these trios should be submerged to a depth not smaller than the typical layer thickness. Figure 11 shows the distribution of 96 vertices of Cf fission into three fragments along the depth of the NTE layer with an average value of (4.1 ± 0.2) μm and an RMS of 2.5 μm. This effect may be due to binding of Cf atoms in AgBr microcrys-

tals and their drift. Probably, the surface protection of the source with an initial thickness of deposited gold of 50 μg/cm^2 (according to the source certificate) was incapable of preventing such penetration.

The ranges of all fragments were measured in 96 events of true tripartition, i.e., without α particles (Fig. 12). The comparison with the data in Fig. 9 indicates that the average energy of fission fragments is about 400 A keV. This, however, is a rough estimate. The calibration of ion ranges in NTE should begin much lower than 1 A MeV in controllable conditions provided by accelerators and ion sources. An efficient criterion of splitting into three heavy fragments is their total range (Fig. 13). The fragment opening angles were also measured in these events (Fig. 13). Their distribution is characterized by an average value of (111 ± 2)° and an RMS of 36°. It can be concluded that no candidates for collinear fission have been found yet, and their search should be continued.

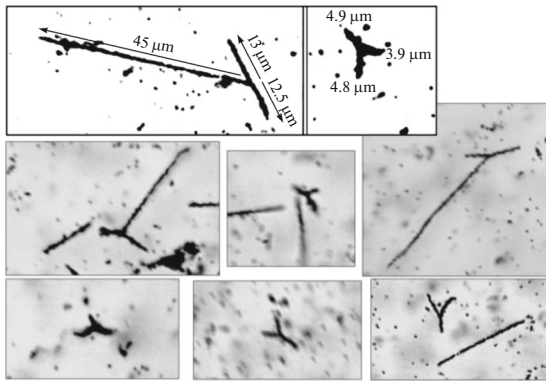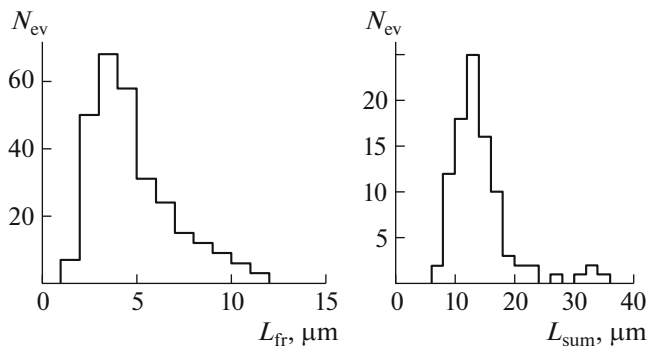**Fig. 10.** Examples of observed tripartition events; in two cases, track lengths are shown.

Fig. 11. Distribution of ^{252}Cf tripartition events over the NTE depth.

Fig. 12. Distributions of ^{252}Cf tripartition events over (left) the fragment range L_{fr} and (right) the range sum in trios L_{sum}.
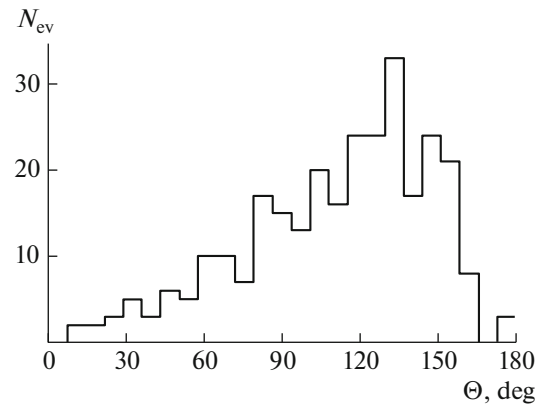
Fig. 13. Distributions of ^{252}Cf tripartition events over opening angles of fragment pairs.

EXPERIENCE OF AUTOMATIC MEASUREMENTS

The capabilities of computer track analysis using the HSP-1000 microscope and the code ImageJ [22] were studied with NTE samples irradiated with heavy ions. The HSP-1000 microscope [23] manufactured by Seiko Precision is equipped with a high resolution linear sensor with an image acquisition rate higher by a factor of 50 than common CCD cameras. The total image of the sample is reconstructed along with continuous picture taking of a relatively small number of long chains. Previously, this microscope was used in analysis of solid state detectors.

Figure 14 shows the stages of detailed analysis of NTE irradiated with Kr ions with an energy of $1.2\,A$ MeV at the IC-100 cyclotron of the Laboratory of Nuclear Reactions (JINR). Several hundred frames were made with the HSP-1000 microscope. Then the parameters of selected tracks were chosen. After that, the code analyzed frames in a sequence. As a result, we obtained the ion range and planar ion incidence angle distributions (Fig. 15). The angular distribution indicates the presence of two charge components of ions.
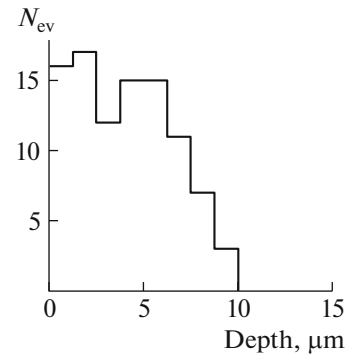
Thus, NTE is quite a useful detector for detailed analysis of ion beams.

IRRADIATION WITH THERMAL NEUTRONS

NTE samples enriched in boron (boric acid and borax) were irradiated for 30 min at the thermal neutron channel of the IBR-2 reactor (JINR). The subsequent sample analysis yielded an intensity estimate of 5×10^5 neutrons per second. The samples were produced by casting boron-enriched NTE to a thickness of about 60 μm onto a 2 mm glass substrate. The application of glass resulted in activation of sodium contained in it, which presented a problem, although inevitable.

The presence of boron in NTE allows one to observe charged products of the $n_{th} + {}^{10}B \rightarrow {}^7Li + (\gamma) + {}^4He$ reaction. This reaction occurring with emission of 2.8 MeV of heat has a probability of 93%; in this reaction, photons with an energy of 478 keV are emitted by the ^{7}Li nucleus from the only excited state. The coordinate measurements of tracks in 112 ^{7}Li + ^{4}He events
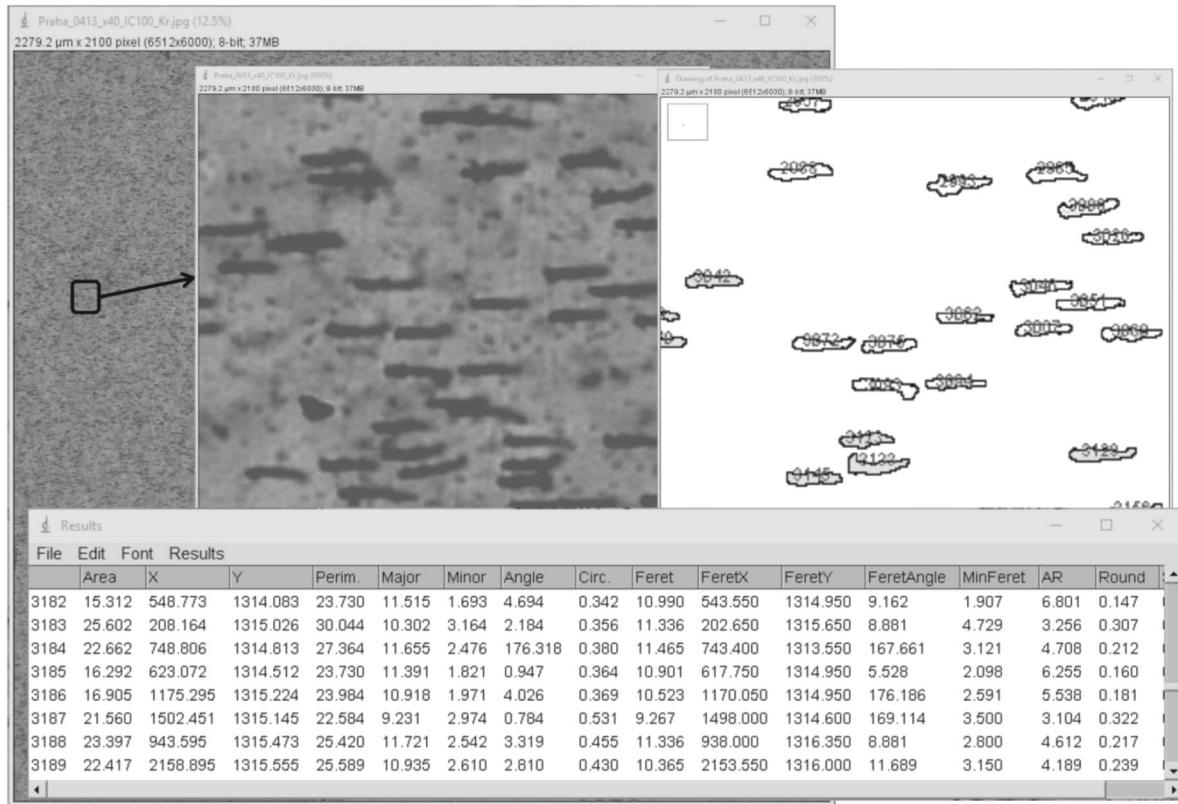
Fig. 14. Illustration of track recognition in the code ImageJ: (background frame) NTE surface scanned with 20-fold magnification after irradiation with 1.2 *A* MeV Kr ions; (central frame) fragment with different tracks; (right) detected objects of interest, enumerated; and output list of parameters of detected objects.
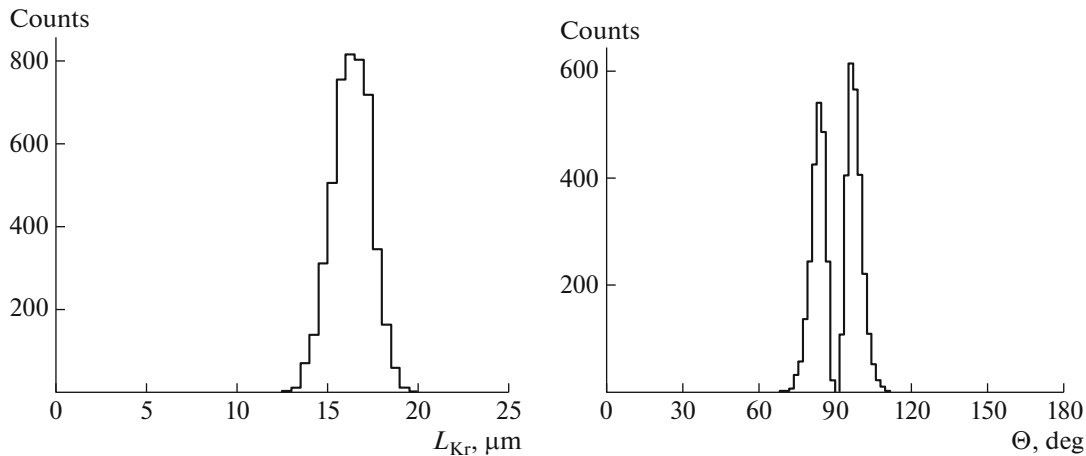

Fig. 15. Result of ImageJ processing: (left) lengths of found tracks of 1.2 *A* MeV Kr ions and (right) their planar angles of incidence to NTE.

were performed. Their directions in pairs are noncollinear and have an average angle $\Theta(^7\text{Li} + {}^4\text{He})$ of $(148 \pm 14)°$ due to photon emission. The average energy $Q(^7\text{Li} + {}^4\text{He})$ was (2.4 ± 0.2) MeV with an RMS of 0.8 MeV in agreement with the energy carried away by the photon. The distribution of $\Theta(\gamma + {}^7\text{Li})$

between the photon emission angles calculated from the momentum conservation and the ^7Li direction point to apparent anticorrelation (Fig. 16).

The experience of computer counting of boron splitting tracks was acquired while scanning with the HSP-1000 microscope. The reconstruction of planar
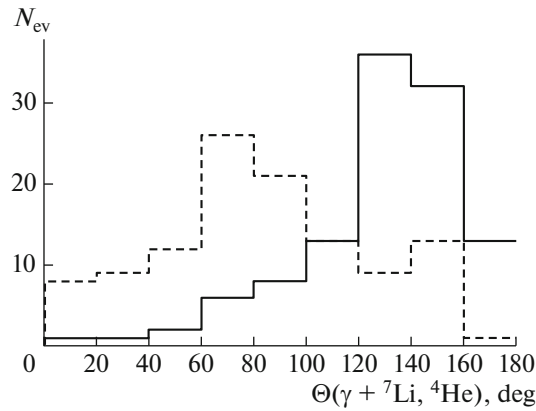
Fig. 16. Distribution over the angles $\Theta(\gamma + {}^7\text{Li},{}^4\text{He})$ between the calculated photon directions and the directions of (solid line) ${}^7\text{Li}$ and (dashed line) ${}^4\text{He}$ nuclei.
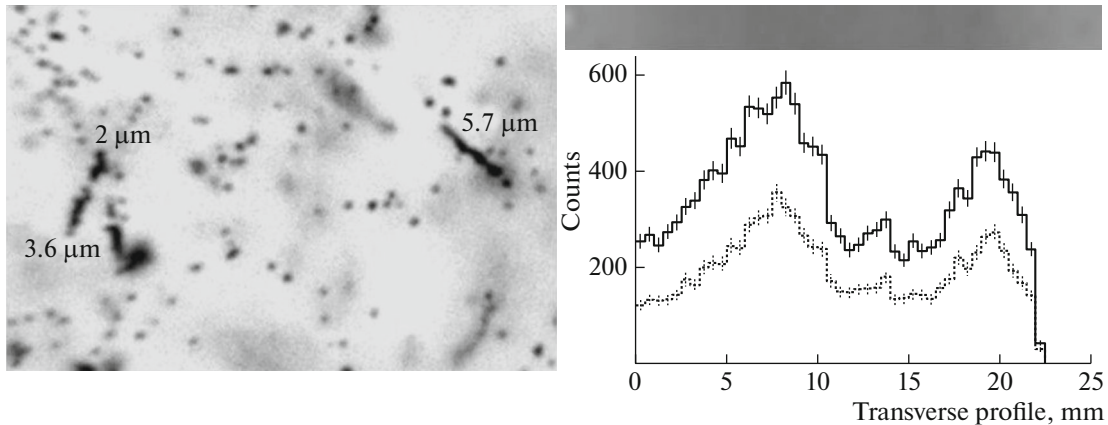

Fig. 17. (Left) macrophoto of typical tracks in boron-enriched NTE irradiated with thermal neutrons; (upper right) 25-mm-long strip scanned at the automatic microscope; (lower right) distribution of (upper) Li + He tracks and (lower) single He tracks along this strip.

Li + He tracks and single He tracks using the code ImageJ [22] allowed one to find up to 16 000 tracks along the scanned strip with a length of 25 mm and a width of 1 mm. These events were used to reconstruct the thermal neutron beam profile (Fig. 17).

CONCLUSIONS

So far, the NTE technique is based on intelligence, eyesight, and efficiency of researchers using traditional microscopes. In spite of broad interest in the capabilities of this method, its cumbersome character results in limited statistics of hundreds of measured tracks, which is, as a rule, a negligibly small part of available events. The application of computerized and completely automated microscopes makes it possible to overcome this difficulty. These complex and expensive devices of shared and even remote use provide unprecedented statistics of nuclear tracks. In order to make this development purposeful, it is necessary to

focus on such topical problems of nuclear physics whose solution can be reduced to simple tasks of recognition and measurement of tracks in NTE solved using existing codes. Thus, the conditions for wide dissemination of this experience could be created.

In particular, the proposed problem of analysis of extremely rare events of tripartition is reduced to finding planar trios of nuclear fragments. Beginning at the common vertex and being randomly directed, their tracks should have a length from 1 to 10 μm. Computer image analysis is capable of selecting appropriate decays for subsequent manual analysis. The automation of the search for tripartition events would reduce sharply the most cumbersome stage and assist in focusing manual analysis on discovered events. Thus, manual and automatic analysis are complementary.

On the whole, the synergy of modern radioactivity sources, verified NTE metrology, and advanced microscopy seems promising for investigation of α

radioactivity and nuclear fission. It can be anticipated that ions of transfermium elements would be implanted in NTE. Pronounced decays of these ions could then be observed as common vertices for several α particles and nuclear fragments. These prospects prove the fundamental value of preservation and improvement of the NTE technique. Thus, this study, focused on reintroducing NTE into the practice of nuclear experiments, would serve as a prototype for solving an impressive amount of problems. The macrophotos of the experiments under discussion and the corresponding videos are available on the website of the BECQUEREL project [4].

REFERENCES

1. C. F. Powell, P. H. Fowler, and D. H. Perkins, *Study of Elementary Particles by the Photographic Method* (Pergamon, London, 1959).

2. W. H. Barkas, *Nuclear Research Emulsions* (Academic, New York, London, 1963).

3. Y. Goldschmidt-Cremont, Ann. Rev. Nucl. Sci., 141 (1953).

4. The BECQUEREL Project. http://becquerel.jinr.ru/.

5. P. I. Zarubin, Lect. Notes Phys. **875** (3), 51 (2014).

6. Slavich Company JSC. http://www.newslavich.com/.

7. D. A. Artemenkov, A. A. Bezbakh, V. Bradnova, M. S. Golovkov, A. V. Gorshkov, P. I. Zarubin, I. G. Zarubina, G. Kaminski, N. K. Kornegrutsa, S. A. Krupko, K. Z. Mamatkulov, R. R. Kattabekov, V. V. Rusakova, R. S. Slepnev, R. Stanoeva, S. V. Stepantsov, A. S. Fomichev, and V. Chudoba, Phys. Part. Nucl. Lett. **10**, 415 (2013).

8. D. A. Artemenkov et al., Few-Body Syst. **55**, 733736 (2014).

9. P. Zarubin, EPJ Web Conf. **66**, 11044 (2014).

10. R. R. Kattabekov, K. Z. Mamatkulov, S. S. Alikulov, D. A. Artemenkov, R. N. Bekmirzaev, V. Bradnova, P. I. Zarubin, I. G. Zarubina, N. V. Kondratieva, N. K. Kornegrutsa, D. O. Krivenkov, A. I. Malakhov, K. Olimov, N. G. Peresadko, N. G. Polukhina, et al., Phys. At. Nucl. **76**, 1219 (2013).

11. D. A. Artemenkov, V. Bradnova, A. A. Zaitsev, P. I. Zarubin, I. G. Zarubina, R. R. Kattabekov, K. Z. Mamatkulov, and V. V. Rusakova, Phys. At. Nucl. **78**, 579 (2015).

12. D. V. Kamanin and Y. V. Pyatkov, Lect. Notes Phys. **875** (3), 184 (2014).

13. K. Z. Mamatkulov et al., Phys. Proc. **74**, 59 (2015).

14. E. W. Titterton and T. A. Brinkley, Nature **187**, 228 (1960).

15. M. L. Muga, H. R. Bowman, and S. G. Thompson, Phys. Rev. **121**, 271 (1961).

16. D. A. Artemenkov, V. Bradnova, A. A. Zaitsev, P. I. Zarubin, I. G. Zarubina, R. R. Kattabekov, N. K. Kornegrutsa, K. Z. Mamatkulov, P. A. Rukoyatkin, V. V. Rusakova, and R. Stanoeva, Phys. At. Nucl. **78**, 794 (2015).

17. F. Ajzenberg-Selove, Nucl. Phys. A **490**, 1 (1988); TUNL—Nuclear Data Evaluation Project. http://www.tunl.duke.edu/NuclData/.

18. The BECQUEREL Project. http://becquerel.jinr.ru/miscellanea/8He/8He.html.

19. F. Ziegler, J. P. Biersack, and M. D. Ziegler, SRIM — the Stopping and Range of Ions in Matter. http://srim.org/.

20. V. M. Bystritsky, V. V. Gerasimov, V. G. Kadyshevsky, A. P. Kobzev, A. R. Krylov, A. A. Nozdrin, V. L. Rapatsky, Yu. N. Rogov, A. B. Sadovsky, A. V. Salamatin, M. G. Sapozhnikov, A. N. Sissakian, V. M. Slepnev, N. I. Zamyatin, and E. V. Zubarev, Phys. Part. Nucl. Lett. **6**, 505 (2009).

21. T. Yamada, Y. Funaki, H. Horiuchi, G. Roepke, P. Schuck, and A. Tohsaki, Lect. Notes Phys. **848** (1), 102 (2012).

22. Image Processing and Analyses in JAVA. http://rsb.info.nih.gov/ij/.

23. Microscope HSP-1000. http://www.odz.ujf.cas.cz/home/resources/microscope-hsp-1000.

Translated by E. Baldina